

# From Green to Grey: Exploring Land Cover Transformation and Urban Heat Island Dynamics in Greater Accra, Ghana

Fosu Enoch Atuahene<sup>1</sup>, Enoch Aninakwah<sup>1,\*</sup>, Isaac Aninakwah<sup>2</sup>, Oteng Tristy Konadu<sup>1</sup>

<sup>1</sup> *Department of Geography and Resource Development University of Ghana, Legon, Ghana*

<sup>2</sup> *Department of Social Sciences St. Monica's College of Education, Mampong, Ashanti, Ghana*

\*Correspondence: [eaninakwah@st.uq.edu.gh](mailto:eaninakwah@st.uq.edu.gh)

Received: 17 Jul 2025; Revised: 17 Aug 2025; Accepted: 1 Sep 2025; Published: 30 Sep 2025

**Abstract:** Urban heat intensification remains a pressing environmental challenge in rapidly growing African cities, yet limited empirical data exist on its spatio-temporal evolution. This study assessed land surface temperature (LST) and Urban Heat Island (UHI) dynamics in the Greater Accra Region between 2010 and 2024 using multi-temporal Landsat imagery, supervised classification, and geospatial analysis in ArcGIS and ENVI. Land cover changes were quantified, and UHI zones were mapped to evaluate the relationship between urbanisation and thermal patterns. Results revealed that built-up areas expanded by approximately 67,850 ha, while vegetation cover declined by over 45%, leading to a marked intensification of UHI. In 2010, UHI values ranged from 2.55 °C to 15.10 °C, rising sharply to 9.20 °C–25.70 °C by 2024, with high-intensity zones covering more than 70% of the landscape. Town-level analysis further indicated that mean LST values exceeded 34 °C in dense urban cores, such as Accra Central and Madina, compared to values below 27 °C in peri-urban and water-adjacent areas. The persistence of cooling effects near water bodies and green clusters highlights their mitigating influence, although their spatial extent continues to shrink. These findings demonstrate that uncontrolled urban expansion directly amplifies surface heating, posing risks to thermal comfort, energy demand, and public health. The novelty of this research lies in its multi-temporal quantification of UHI escalation over 14 years in Accra, providing robust evidence for integrating vegetation restoration, green roofs, and sustainable urban design into planning. Future studies should refine predictive models and incorporate socio-economic variables to strengthen climate resilience strategies.

**Keywords:** Urban Heat Island; Land Cover Change; Land Surface Temperature; Greater Accra; Urbanisation

## 1.0 Introduction

Urbanisation is one of the most significant global phenomena of this century. Rapid urbanisation has driven socio-economic advancement, including the development of urban infrastructure, improvements in transportation systems, and enhanced healthcare (Athukorala & Murayama, 2020). However, anthropogenic activities associated with urbanisation reduce vegetated and green spaces, thereby increasing impervious surfaces in cities. This, in turn, raises urban surface temperatures relative to rural regions, resulting in the formation of Urban Heat Islands (UHIs) (Devendran & Banon, 2022). Climate change in and around cities is strongly influenced by land use/land cover (LULC) changes and anthropogenic activity (Borsah et al., 2025).

The urban environment in Ghana has expanded significantly over the last decade due to population growth and rural-urban migration, strongly impacting land use, land cover, and overpopulation (C. Wemegah, 2020; Aninakwah et al., 2024). Greater Accra is the most urbanised region in Ghana (C. S. Wemegah et al., 2020a) and has experienced extensive LULC changes driven by urbanisation (Frimpong et al., 2023). Recent studies indicate that built-up expansion in Accra is among the fastest in West Africa, with vegetation cover declining by more than 40% over the past two decades (Reagan et al., 2023; Biney et al., 2024). Urban growth is often accompanied by uncontrolled LULC changes for development activities such as industrialisation, road construction, and the erection of buildings using high thermal-capacity materials, which create impervious surfaces (Aninakwah & Aninakwah, 2025). These modifications alter the natural environment, changing the surface energy budget (SEB) and promoting the formation of UHIs (C. S. Wemegah et al., 2020b). UHIs result from higher land surface temperatures in urban areas compared to surrounding rural areas (Athukorala & Murayama, 2020).

UHIs are generally associated with elevated LST. Urban geometry, construction materials, and changes in land cover are key contributors to this phenomenon (Biney et al., 2024). UHIs typically emerge when natural vegetation is replaced by dense concentrations of heat-absorbing materials—such as concrete buildings, asphalt roads, iron roofing sheets, block pavements, and other impervious surfaces—during urbanisation. These materials absorb and emit heat, increasing LST and contributing to higher air temperatures and global warming (Reagan et al., 2023). Tropical cities such as Accra are particularly vulnerable, as rising LST intensifies energy demand for cooling and exacerbates urban health risks (Asori & Adu, 2023). Climate change, with its associated rise in average temperatures, further amplifies the UHI effect in tropical urban settings (Gyasi-Addo). Abnormally high LSTs in cities can increase the incidence of heat-related illnesses, including heat stress, heat cramps, and heatstroke (Asori & Adu, 2023).

Surface Urban Heat Islands (SUHIs) have wide-ranging effects on urban health. Evidence suggests a link between UHI intensity, reduced labour productivity, and increased public health costs in African cities (Mensa et al., 2020). For example, over 14,000 deaths in France in 2003 were attributed to heatwaves, and studies in Allahabad, India, reported a 40% increase in mortality in May 2010 when temperatures exceeded 45 °C (Buo, 2019). UHIs, particularly noticeable at night and during summer, contribute to thermal discomfort and adversely affect human, animal, and plant health, as well as energy consumption and productivity (Mensah et al., 2020). In Ghana, outdoor workers are particularly at risk from urban heatwaves—a concern likely to worsen as over 51% of the population currently lives and works in cities (Asori & Appiah, 2022). Given this context, studying UHI in Greater Accra is crucial for quantifying its magnitude, spatial extent, and health implications, and for providing evidence to inform adaptation strategies. Assessing UHI warming can guide the development of early warning systems and policies to mitigate its adverse effects.

### 1.1. Statement of Scientific Interest

Urbanisation is a global phenomenon with significant environmental implications, particularly for temperature dynamics within urban areas (Frimpong, Agyei, & Mensah, 2023). The Urban Heat Island (UHI) phenomenon arises from differences in air temperature between urban areas and their surrounding rural regions (Gyasi-Addo, 2021). The Greater Accra Region is the most urbanised area in Ghana, and over the past decade, it has experienced rapid population growth and urban sprawl. These changes have altered the natural environment, leading to the formation and intensification of UHI. The presence of UHI can elevate both air and land surface temperatures (LST), adversely affecting the urban microclimate and energy consumption. It can also increase concentrations of air pollutants and greenhouse gases, further impacting

human health and comfort (Wemegah et al., 2020a). Previous studies, however, have not provided sufficient evidence of UHI presence in the region (Wemegah, 2020).

This study aims to investigate land cover changes and the spatial extent of UHI in the Greater Accra Region from 2010 to 2024. The following hypotheses were tested:

1. UHI effects are more pronounced in areas with high population density.
2. The replacement of vegetated areas with built-up structures, including paved surfaces and tarred roads, contributes significantly to the occurrence of UHI effects.
3. Regions with abundant vegetation and proximity to water bodies exhibit lower temperatures compared to inland areas lacking these features.

## 2.0 Literature Review

Urban Ecology Theory was introduced by thinkers such as Robert Park, Ernest Burgess, and Roderick McKenzie. They conceptualised the city as an organism, constantly growing, evolving, and adapting to its inhabitants. The theory explains how people migrate to cities, compete for space, and gradually transform land use. Over time, farms and forests are replaced by houses, roads, and major buildings. It also suggests that as cities expand, they pass through natural stages, with some areas becoming dense and crowded while others remain quieter or undergo significant transformation. The theory thus links human activity with the physical changes occurring in urban environments.

Urban Ecology Theory is particularly relevant for studying land cover changes and urban heat in the Greater Accra Region. As Accra expands, green spaces are increasingly replaced by concrete structures and buildings. According to the theory, this process is a natural part of urban development. However, it also explains why certain parts of the city experience higher temperatures due to the reduction of vegetation and the proliferation of heat-retaining surfaces. Consequently, the theory provides a framework for understanding not only what changes are occurring in Accra but also why they are happening. It illustrates the connection between land use practices and environmental outcomes, such as elevated temperatures in urban neighbourhoods. This theoretical perspective, therefore, underpins the linkage between spatial transformations (land cover loss) and environmental consequences (UHI intensity), justifying its application to the Accra case.

### 2.1 Concept of UHI

An Urban Heat Island (UHI) refers to the temperature difference between urban areas and their surrounding rural regions. This phenomenon primarily arises from changes in land use and land cover, particularly the conversion of vegetated surfaces into impervious surfaces, which leads to increased land surface temperatures in metropolitan areas (Borsah, Mensah, & Owusu, 2024). UHI is observed both during the day and at night but is typically more pronounced at night. During daylight hours, rural areas cool more rapidly due to higher evapotranspiration, whereas urban areas retain heat for longer periods, resulting in significant nighttime temperature differences. Consequently, differences in minimum (nighttime) temperatures between urban and rural areas are considered primary indicators of UHI intensity (Wemegah, 2020). According to Gyasi-Addo (2020), UHI arises from microclimatic alterations caused by human-induced surface changes and anthropogenic heat emissions.

### 2.2 Causes of Urban Heat Island (UHI)

Past studies have identified vegetation, roads, open spaces, and hardscape as key factors contributing to variations in the urban climate. However, roads have been shown to be the most significant contributor to UHI (Gyasi-Addo, 2021). The conversion of vegetated areas into impervious surfaces, such as roads and buildings, combined with industrial and economic growth associated with urbanisation, significantly increases land surface temperatures (LST) due to reduced evapotranspiration and increased heat absorption (Borsah, Mensah, & Owusu, 2024). The use of high-thermal-capacity materials, including concrete, asphalt, and metal, further intensifies UHI by retaining and emitting heat (Wemegah, Sarpong, & Appiah, 2020).

The replacement of green spaces with urban landscapes diminishes natural cooling mechanisms, resulting in elevated urban temperatures (Athukorala & Murayama, 2020). Devendran and Banon (2022) highlight that transforming natural landscapes, such as forests and agricultural lands, into impervious urban surfaces is a primary driver of UHI, significantly altering the surface energy balance. The spatial expansion of urban areas further intensifies this phenomenon, with studies demonstrating a direct correlation between built-up areas and higher land surface temperatures (Frimpong, Agyei, & Mensah, 2023). According to Wemegah (2020), urban growth in Greater Accra, coupled with anthropogenic activities such as vehicle emissions and industrial heat release, exacerbates UHI effects. Remote sensing indices, such as the Normalized Difference Vegetation Index (NDVI), provide evidence of declining vegetation cover, confirming the intensification of surface warming in urbanised zones.

### 2.3 Effects of Urban Heat Island

Studies have shown that increased UHI can affect energy use, both for heating and cooling, in urban buildings (Gyasi-Addo, 2021). Rising UHI may also alter precipitation patterns, increase demand for energy and air conditioning, and elevate pollution levels, contributing to global warming and negatively affecting environmental quality (Biney, Mensah, & Ofori, 2024). Higher land surface temperatures (LST) adversely impact local climate conditions, and economically, cities may incur substantial financial losses as ecosystem services, including hydrological services, degrade (Asori & Adu, 2023).

UHI has wide-ranging effects on the health of urban residents. It can intensify concentrations of air pollutants and greenhouse gases, thereby affecting human health and comfort (Wemegah, Sarpong, & Appiah, 2020). Globally, UHI-related health impacts include heat exhaustion, general discomfort, respiratory difficulties, heatstroke, and other heat-related morbidities and mortalities (Reagan, Kofi, & Agyemang, 2023). For instance, over 14,000 deaths in France in 2003 were attributed to heatwaves (Buo, 2019). In Allahabad, India, mortality in May 2010 increased by 40% compared to the average of previous years when temperatures exceeded 45 °C (Buo, 2019). Health issues such as stroke, thermal exhaustion, cardiovascular problems, and respiratory diseases are among the many detrimental effects of UHI. Efforts to improve indoor comfort for building occupants may also have unintended consequences on the microclimate (Gyasi-Addo, 2021).

In African cities, vulnerability to UHI is particularly pronounced due to limited adaptation infrastructure, with outdoor workers, informal settlers, and the elderly being most at risk (Mensah, Frimpong, & Owusu, 2020). Thus, UHI represents not only an environmental concern but also a socio-economic and public health challenge.

### 3.0 Materials and Methodology

### 3.1 Study Area

This study was conducted in the capital city of Ghana, the Greater Accra Region (Figure 1). The region covers a total area of 3,245 square kilometres and is located along the Atlantic coast of West Africa. Its coastline extends 225 km, from Kokrobite in the west to Ada in the east. The area falls within a dry coastal equatorial climate zone, with temperatures ranging from 20 °C to 30 °C and annual rainfall varying from 635 mm along the coast to 1,300 mm in the northern parts (Borsah, Mensah, & Owusu, 2024). Accra experiences a bimodal rainfall pattern, with annual precipitation ranging from approximately 780 mm to 1,200 mm. The main rainy season begins in April, peaking between May and August, while the minor season occurs from October to November (Wemegah, 2020).

The Greater Accra Region was selected for this study because it is the most densely populated, industrialised, and commercial region in Ghana (Wemegah, Sarpong, & Appiah, 2020). Accra serves as a centre of economic and administrative activity and is a popular tourist and cultural hub, offering a wide array of hotels, restaurants, and nightclubs. Residents work across diverse sectors, including offices, factories, artisan trades, and commerce (Borsah et al., 2024).

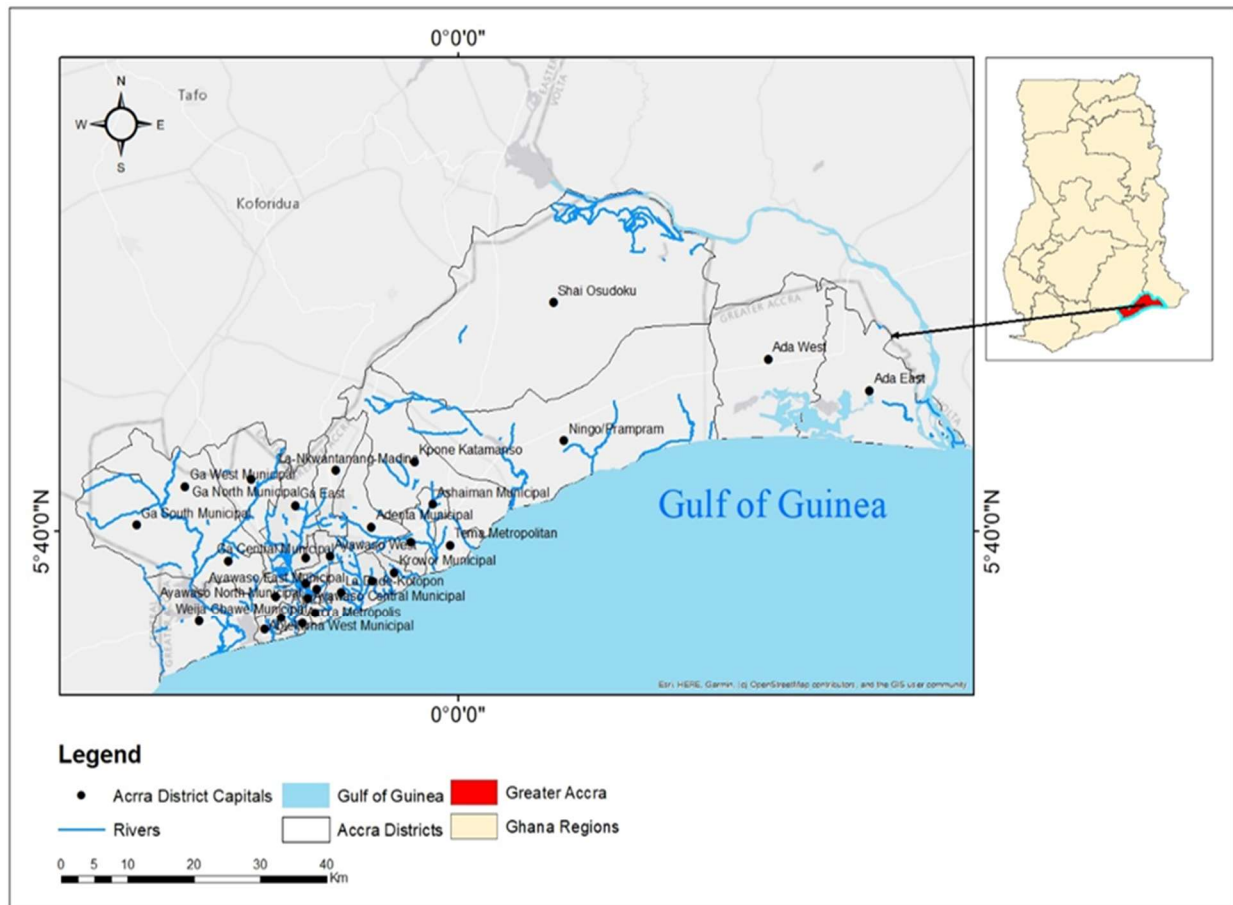


Figure 1: Study Area Map  
Source: Author's Construct (2025)

### 3.2 Research Design

This study employed a spatio-temporal research design to examine land cover transformation and Urban Heat Island (UHI) dynamics in the Greater Accra Region. Multi-temporal satellite imagery, geospatial analysis, and land cover classification techniques were used to quantify changes in vegetation and built-up areas, and to assess their influence on surface temperature patterns over time, as shown in Figure 2.

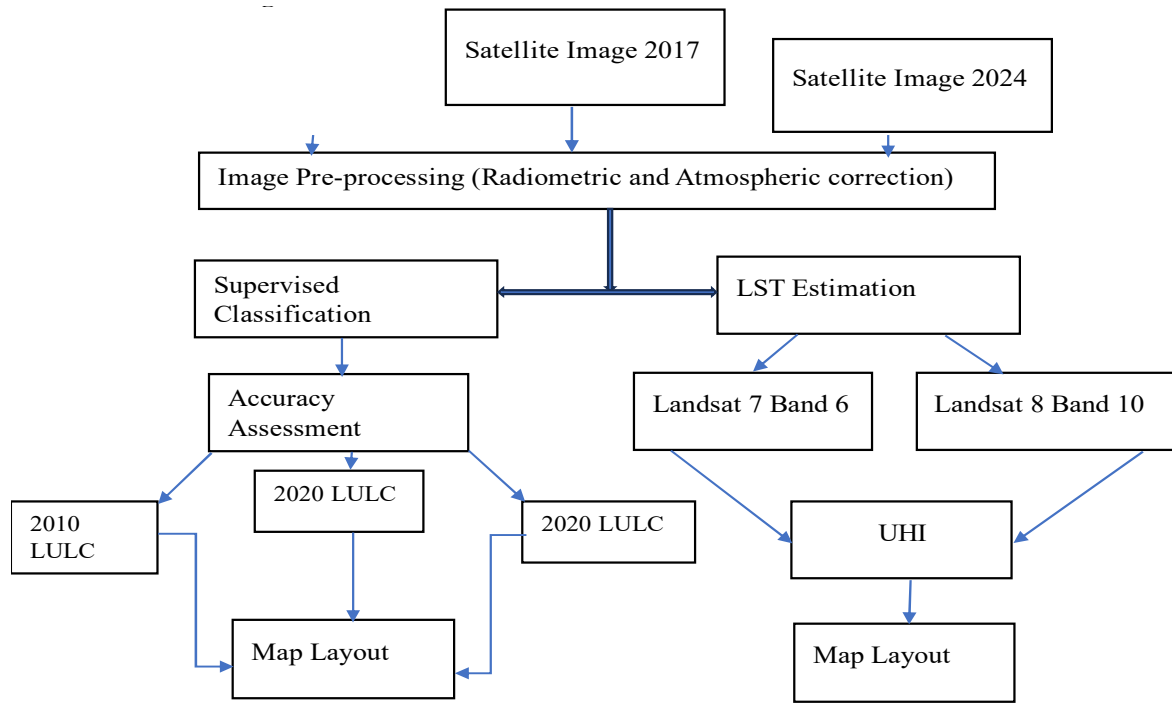


Figure 2. Research Design  
Source: Author's Construct (2025)

### 3.3 Image Pre-processing and Classification

Satellite images are often affected by distortions during the imaging process and therefore require correction before further processing and analysis (Biney, Mensah, & Ofori, 2024). In this study, radiometric and geometric corrections were applied to the acquired Landsat images using ENVI 5.3 software. The maximum likelihood classifier (MLC) algorithm was employed to map land cover types, and a supervised classification method was used to categorise the images into four distinct classes.

Specifically, the four classes considered in this study were built-up areas, vegetation, bare soil, and water bodies, reflecting the land cover conditions in the Greater Accra Region. Pre-processing was conducted prior to retrieving land surface temperature (LST). Atmospheric correction and radiometric calibration involved converting digital number (DN) values from the satellite data, including (1) multispectral bands to surface reflectance and (2) thermal bands to satellite brightness temperature. The spectral radiance (LA) was derived for Landsat 7 ETM+ and Landsat 8 OLI/TIRS from the quantised calibrated pixel values. These pre-processing steps ensured consistency across sensors and years, which is critical for accurate spatio-temporal comparison of LST (Roy, Ju, & Zhang, 2014; Li, Li, & Liu, 2020).

### 3.4 Satellite Imagery

The study utilised two satellite sensors to acquire three images: Landsat 7 Enhanced Thematic Mapper Plus (ETM+) for the 2010 image, and Landsat 8 Operational Land Imager (OLI) combined with the Thermal Infrared Sensor (TIRS) for the 2017 and 2024 images. Further details of these images are provided in Table 1. All images were obtained from the Landsat satellite products provided by the U.S. Geological Survey (USGS).

To minimise the influence of cloud cover and seasonal variability, all images were selected from the dry season months. Landsat data offer a spatial resolution of 30 m for multispectral bands and 100 m (resampled to 30 m) for thermal bands, making them suitable for LST retrieval and urban studies (Chander, Markham, & Helder, 2009). For this study, images were acquired across various spectral bands, as detailed in Table 2. Additionally, the land cover classifications and their respective emissivity values used for estimating LST are listed in Table 3.

Table 1. Landsat Image Data Acquired for the Study

Sensor	Spatial Resolution	Date Acquired	Scene Time	Cloud cover	Sun Azimuth	Sun Elevation
Landsat 7 ETM	30m	2010-01-30	10:07:25am	20.00%	127.563%	51.058%
Landsat 8 OLI	30m	2017-01-25	10:15:47am	1.12%	131.315%	52.168%
Landsat 8 OLI	30m	2024-01-29	10:15:43am	26.34%	130.037%	52.545%

Table 2. Spectral Band Details for Landsat 7 and 8 from (Wemegah, 2020)

Band Number	Band Name		Wavelength (μ m)	
	Landsat 7	Landsat 8	Landsat 7	Landsat 8
1	Blue	Coastal aerosol	0.4 - 0.52	0.43 - 0.45
2	Green	Blue	0.53 - 0.6	0.45 - 0.51
3	Red	Green	0.63 - 0.69	0.53 - 0.59
4	NIR	Red	0.76 - 0.90	0.64 - 0.67
5	SWIR	NIR	1.55 - 1.75	0.85 - 0.88
6	TIR/TIR1, TIR2	SWIR1	10.40 - 12.50	1.57 - 1.65
7	SWIR2	SWIR2	2.08 - 2.35	2.11 - 2.29
8	X/Pancromatic	Pancromatic	X/0.52 - 0.90	0.50 - 0.68
9	X	Cirrus	X	1.36 - 1.38
10	X	TIR1	X	10.60 - 11.19
11	X	TIR2	X	11.50 - 12.51

Table 3. Land Cover Classification and its Emissivity (Wemegah, 2020)

Class ID	Macro-class Name (Land surface type)	Emissivity(e)	Color ID
1	Built-Up	0.94	Ash
2	Vegetation	0.98	Green
3	Bare Land	0.93	Yellow
4	Water	0.98	Blue

### 3.5 Data Processing and Land Surface Temperature

The data were processed using computer software developed by the Environmental Systems Research Institute (ESRI). ArcGIS 10.8.2, ENVI 5.3, and QGIS 3.34.15. The land surface temperature of the two respective years was Quantified using the raster calculator in ArcMap 10.8.2. Band 6 of Landsat 7 ETM+ was used as the thermal band to quantify the LST of the year 2010, and band 10 of Landsat-8 was used to quantify the LST for the years 2017 and 2024. According to Nagbija (2022), the first step in quantifying the LST is to convert the top-of-atmosphere (TOA) radiance. Using the radiance rescaling factor, the thermal infrared digital numbers can be converted to TOA spectral radiance using the equation  $TOA(L) = M_L \cdot Q_{Cal} + A_L$  in the raster calculator.

After the TOA is calculated, the next step will be to convert it to the top of the atmosphere brightness temperature (BT). Using the equation  $BT = (K_2 / (\ln(K_1/L) + 1) - 273.15)$ , the spectral radiance data can be converted to the top of the atmosphere brightness temperature using the thermal constant values in the metadata file of the satellite image.

The third step involves the Normalised Vegetation Index (NDVI), which can be quantified using the equation  $NDVI = (Band\ 5 - Band\ 4) / (Band\ 5 + Band\ 4)$ . In the case of Landsat 7 ETM+ bands, bands 3 and 4 will be used. After the NDVI is calculated, the following parameter is land surface emissivity, and this can be calculated using the formula  $P_v = \text{Square}((NDVI - NDVI_{min}) / (NDVI_{max} - NDVI_{min}))$  formulae. This refers to the emissivity of the elements on the earth's surface and can be calculated from the NDVI values from the formulae above. The absolute land surface emissivity can be quantified using  $\epsilon = 0.004 \times P_v + 0.986$ . All these parameters will help quantify the land surface temperature LST. The LST of the study area can be quantified with the expression  $LST = (BT / (1 + (0.00115 \times BT / 1.4388) \times \ln(\epsilon)))$ , where BT and  $\epsilon$  are the brightness temperature and land surface emissivity, respectively.

The Urban Heat Island was estimated from the mean and standard deviation of the land surface temperature results for the three consecutive years, 2010, 2017, and 2024.

$$UHI = \frac{LST - LST_m}{SD}$$

Where;

Where, UHI = Urban Heat Islands; LST = Land Surface Temperature;  $LST_m$  = The mean temperature for the study area; SD = Standard Deviation for the temperature

## 4.0 Results

### 4.1 The extent of land cover changes

The LULC analysis from 2010 to 2024 reveals substantial transformations in land cover distribution, as shown in Figure 3. Built-up areas increased from 209,602 hectares (56.47%) in 2010 to 237,615 hectares (64.05%) in 2017, and further to 277,452 hectares (74.79%) in 2024, representing a total increase of 67,850 hectares over 14 years. In contrast, vegetation cover declined from 100,181 hectares (27.00%) in 2010 to 72,331 hectares (19.49%) in 2017, and then to 59,907 hectares (16.14%) in 2024, resulting in a total loss of 40,274 hectares. Bare land also exhibited a decreasing trend, falling from 49,899 hectares (13.45%) in 2010 to 46,250 hectares (12.47%) in 2017, and then sharply to 19,026 hectares (5.13%) in 2024, marking a loss of 30,873 hectares. Water bodies experienced minor fluctuations, increasing from 11,451 hectares (3.09%) in 2010 to 14,899 hectares (4.01%) in 2017, before slightly declining to 14,760 hectares (3.98%) in 2024.



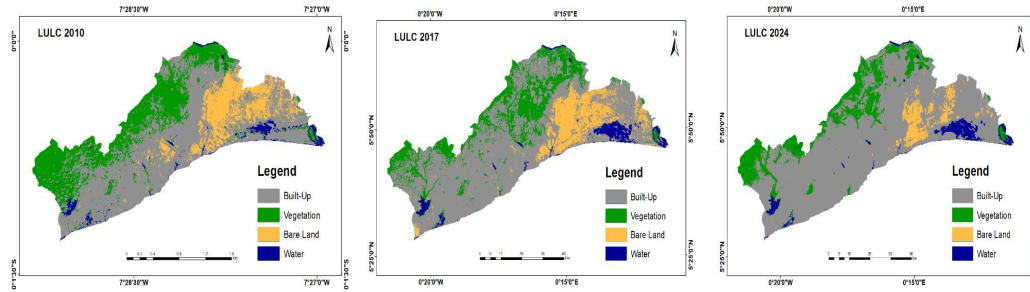


Figure 3: Land us maps from 2010 to 2024

Table 4. The extent of land cover changes from 2010 to 2024

Land Cover Class	Land Cover Change					
	2010		2017		2024	
	Area (Ha)	Area (%)	Area (Ha)	Area (%)	Area (Ha)	Area (%)
Built-Up	209,602	56.47	237,615	64.05	277,452	74.79
Vegetation	100,181	27	72,331	19.49	59,907	16.14
Bare land	49,899	13.45	46,250	12.47	19,026	5.13
Water	11,451	3.09	14,899	4.01	14,760	3.98

#### 4.2. Accuracy Assessment

Tables 5-8 summaris the land cover classification accuracy assessment for 2010, 2017, and 2024. Overall accuracy increased from 80% in 2010 to 90% in 2017 but then declined to 83.3% in 2024. The kappa coefficient, which measures classification reliability, exhibited a similar trend, reaching its highest value of 0.87 in 2017 and its lowest of 0.73 in 2010. These results indicate that the classification was most consistent and reliable in 2017. The decrease in accuracy and kappa in 2024 suggests possible misclassifications or increased spectral confusion among land cover classes.

Table 5: Accuracy assessment for land use map 2010.

2010	Built-Up	Vegetation	Bare Land	Water	Total (User)
Built-Up	5	1	2	0	8
Vegetation	0	8	0	1	9
Bare Land	1	0	6	0	7
Water	0	1	0	5	6
Total (Producer)	6	10	8	6	30

Table 6: Accuracy assessment for land use map 2017.

2017	Built-Up	Vegetation	Bare Land	Water	Total (User)
Built-Up	5	1	0	0	6
Vegetation	0	8	0	0	8
Bare Land	2	0	6	0	8
Water	0	0	0	8	8
Total (Producer)	7	9	6	8	30

Table 7: Accuracy assessment for land use map 2024

2024	Built-Up	Vegetation	Bare Land	Water	Total (User)
Built-Up	6	1	2	0	9
Vegetation	0	5	2	0	7
Bare Land	0	0	6	0	6
Water	0	0	0	8	8
Total (Producer)	6	6	10	8	30

Table 8: Overall Accuracy and Kappa Coefficient

Year	Overall Accuracy	Kappa Coefficient
2010	0.80 (80%)	0.73
2017	0.90 (90%)	0.87
2024	0.833 (83.3%)	0.78

#### 4.3. Change Detection Statistics

According to Figure 4, between 2010 and 2017, 20% of built-up land was converted to other land cover types, while 49.669% of vegetation, 39.752% of bare land, and 3.091% of water bodies also experienced change. The image comparison indicates a 13.365% increase in built-up areas, a 27.800% decrease in vegetation, and a 4.010% increase in water bodies. From 2017 to 2024, as shown in Figures 5 and 6, 8.683% of built-up areas were lost to other land covers, while 40.908% of vegetation, 62.122% of bare land, and 0.081% of water bodies underwent conversion, resulting in a 16.765% increase in built-up areas. Over the entire 2010–2024 period (Fig. 8), 9.476% of built-up areas, 50.497% of vegetation, 74.065% of bare land, and 3.980% of water bodies were converted, corresponding to an overall 32.371% increase in built-up areas, a 40.201% decline in vegetation, and minor fluctuations in water bodies.

Change Detection Statistics (Initial State: 193056\_2010\_Classification.dat, Final State: 193056\_2017...

File Options Help

Pixel Count Percentage Area (Square Meters) Reference

	Initial State					Row Total	Class Total
	Built-Up	Vegetation	Bare Land	Water			
Unclassified	0.016	0.039	0.008	0.128	0.016	100.000	
Built-Up	80.000	48.619	38.771	16.205	99.989	100.000	
Vegetation	10.064	50.331	0.947	2.866	99.981	100.000	
Bare Land	7.370	0.505	60.248	2.028	99.995	100.000	
Water	2.550	0.506	0.026	78.773	99.908	100.000	
Class Total	100.000	100.000	100.000	100.000			
Class Changes	20.000	49.669	39.752	21.227			
Image Difference	13.365	-27.800	-7.312	30.111			

Final State

Figure 4: Changes in Land Cover from 2010 to 2017

Change Detection Statistics (Initial State: 193056\_2017\_Classification.dat, Final State: 193056\_2024...

File Options Help

Pixel Count Percentage Area (Square Meters) Reference

	Initial State					Row Total	Class Total
	Built-Up	Vegetation	Bare Land	Water			
Unclassified	0.003	0.034	0.003	0.091	0.008	100.000	
Built-Up	91.317	40.267	64.149	10.856	99.979	100.000	
Vegetation	7.081	59.092	0.071	1.875	99.955	100.000	
Bare Land	1.050	0.001	35.740	0.008	99.999	100.000	
Water	0.549	0.606	0.037	87.171	99.923	100.000	
Class Total	100.000	100.000	100.000	100.000			
Class Changes	8.683	40.908	64.260	12.829			
Image Difference	16.765	-17.176	-58.863	-0.935			

Final State

Figure 5: Changes in Land Cover from 2017 to 2024.

Change Detection Statistics (Initial State: 193056\_2010\_Classificaion.dat, Final State: 193056\_2024\_Classification.dat)

File Options Help

Pixel Count Percentage Area (Square Meters) Reference

		Initial State					
		Built-Up	Vegetation	Bare Land	Water	Row Total	Class Total
Final State	Unclassified	0.000	0.034	0.002	0.078	0.010	100.000
	Built-Up	90.524	49.596	71.208	21.363	99.983	100.000
	Vegetation	4.679	49.503	0.043	4.155	99.982	100.000
	Bare Land	2.194	0.078	28.730	0.118	100.000	100.000
	Water	2.597	0.788	0.016	74.287	99.913	100.000
Class Total		100.000	100.000	100.000	100.000		
Class Changes		9.476	50.497	71.270	25.713		
Image Difference		32.371	-40.201	-61.871	28.894		

Figure 6: Changes in Land Cover from 2010 to 2024

#### 4.4. Land Surface Temperature

Land Surface Temperature (LST) dynamics for 2010, 2017, and 2024 reveal significant variations across different towns in the study area. The thermal landscape shows a marked increase in temperature, particularly in urban and peri-urban areas, as shown in Figure 7. In 2010, relatively lower temperatures were observed in towns such as Nsawam, Dodowa, and Ada Foah, with LST values ranging from 9.80 °C to 23.35 °C (Figure 8). In contrast, Accra and Ashaiman recorded comparatively higher temperatures, with LST values exceeding 26.75 °C. By 2017, elevated temperatures had extended to areas including Pokuase, Madina, and Amasaman, with LST values ranging from 24.25 °C to 29.80 °C. Cooler regions, such as Oyarifa, Doryumu, and Abokobi, maintained moderate temperatures but showed a gradual warming trend. The 2024 analysis depicts an intensified thermal landscape, with towns such as Lartebikorshie, Dansoman, and Weija experiencing LST values between 32.96 °C and 38.60 °C. Coastal towns, including Nungua, Sakumono, and Teshie, recorded elevated temperatures, while eastern areas such as Tsopoli, Sege, and Koluedor also exhibited rising LST values. The comparative assessment of LST for 2010, 2017, and 2024 highlights a steady increase in land surface temperatures across multiple towns, with the most pronounced changes occurring in highly urbanised and rapidly developing areas (Figure 9).

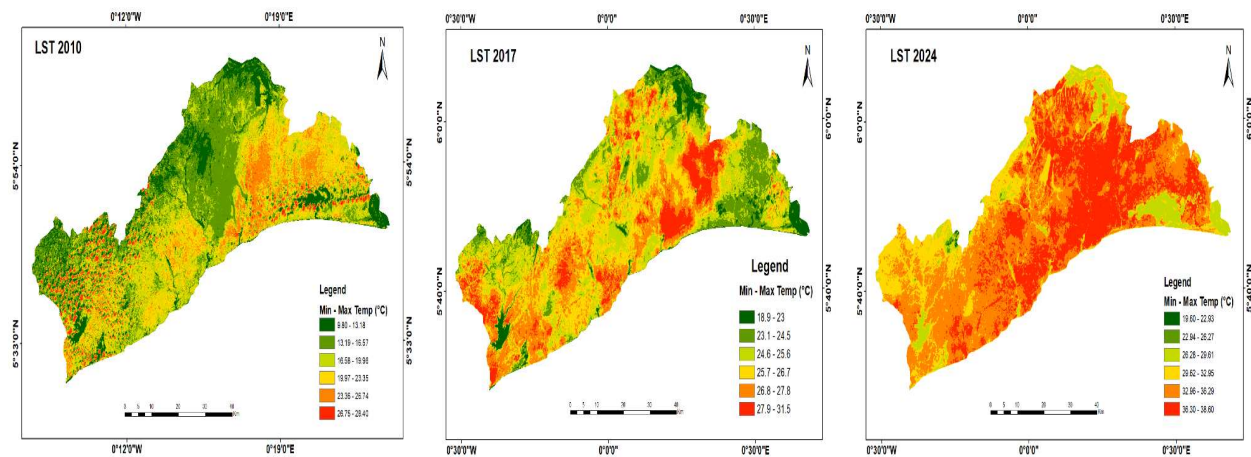


Figure 7: Land Surface Temperature Map of 2020, 2017 and 2024.  
 Source: Author's Construct (2025)



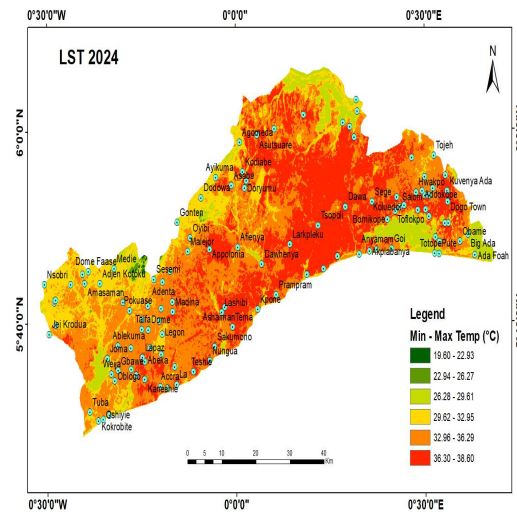


Figure 8 Land Surface Temperature (LST) Distribution across Selected Towns in Accra  
 Source: Author's Construct (2025)

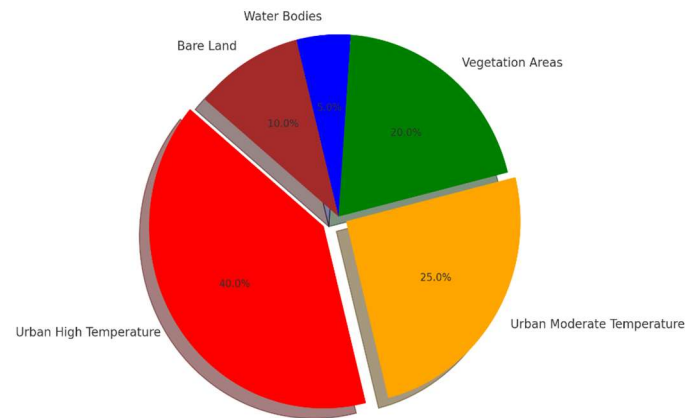


Figure 9. Portion Land Cover Affected by Temperature Variations  
 Source: Author's Construct (2025)

#### 4.5 Urban Heat Island

The UHI maps from 2010, 2017, and 2024 illustrate a significant increase in heat intensity over time, as shown in Figures 10 and 11. In 2010, lower UHI values (2.55 °C – 5.89 °C) were more prominent, especially in forested and water-dominated regions, while higher UHI values (12.75 °C – 15.10 °C) were concentrated in urbanised areas. By 2017, UHI intensity had increased, with high values (16.57 °C–19.20 °C) expanding into previously moderate regions. In 2024, UHI values ranged from 9.20 °C to 25.70 °C, indicating a significant increase in heat retention, with high values predominating across most of the landscape. The once cooler regions were reduced to only a few patches of low UHI values near water bodies and limited green spaces. The comparative analysis from 2010 to 2024 reveals a significant increase in UHI, with higher values becoming increasingly widespread across the study area.

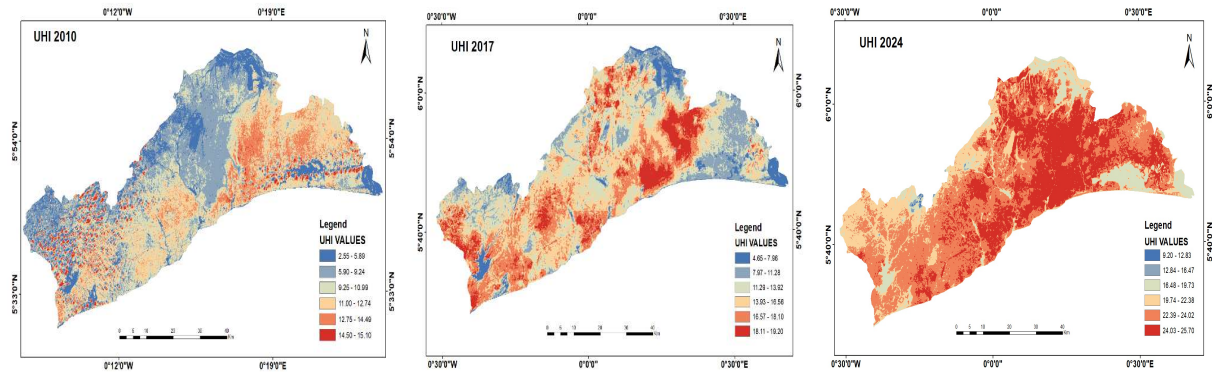


Figure 10 Urban Heat Island (UHI) Maps for 2010, 2017 and 2024.

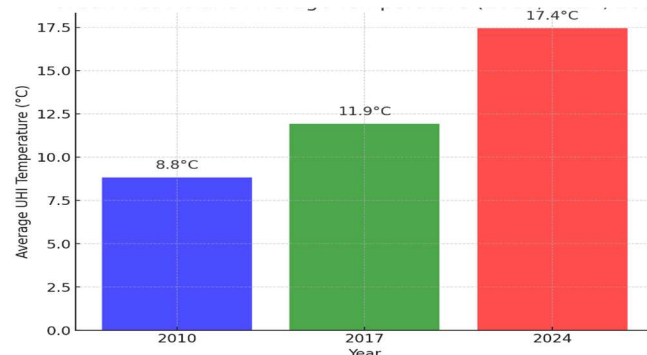


Figure 11 Urban Heat Island (UHI) Average Temperatures for 2010, 2017, and 2024.  
 Source: Author's Construct (2025)

## 5.0 Discussion

The analysis of land use/land cover (LULC), land surface temperature (LST), and urban heat island (UHI) dynamics between 2010 and 2024 provides clear evidence of accelerating environmental transformation in the study area. The findings indicate that urbanisation has emerged as the dominant force shaping the landscape, with profound implications for ecological systems and human well-being (Aninakwah et al., 2025). These results are consistent with earlier studies in Ghana and across sub-Saharan Africa, where rapid urban sprawl has been linked to vegetation loss, microclimatic warming, and intensified heat stress (Acheampong et al., 2021; Forkuor et al., 2020).

The LULC results highlight significant shifts, with built-up areas expanding by over 67,000 hectares, accompanied by a 40% decline in vegetation cover. This transformation was most pronounced between 2017 and 2024, during which built-up land increased by 16.7% while vegetation declined by more than 40%. Bare land diminished sharply, reflecting intensified development projects and reclamation efforts, whereas water bodies showed only minor fluctuations. These observations align with the findings of Athukorala and Murayama (2020), who reported similar vegetation declines across peri-urban Ghana, and Opoku-Ware (2029), who noted the displacement of agricultural lands by expanding cities. The conversion of natural land into impervious surfaces not only disrupts ecological balances but also reduces the landscape's capacity to buffer against heat and hydrological extremes.

The LST analysis further demonstrates the thermal consequences of these changes. In 2010, towns with abundant vegetation and proximity to water, such as Nsawam, Dodowa, and Ada Foah, recorded cooler LST values (9.80°C–23.35°C), whereas dense urban centres, including Accra and Ashaiman, already showed temperatures above 26.75°C. By 2017, peri-urban towns like Pokuase and Amasaman, which were once moderately cool, experienced increased temperatures between 24.25°C and 29.80°C as they rapidly urbanised. By 2024, extreme hotspots emerged in heavily urbanised zones such as Dansoman and Weija, with values exceeding 38°C. This trend confirms the urban heat island effect, where built-up areas composed of impervious materials, such as asphalt and concrete, absorb and retain heat. Similar patterns have been observed in Nairobi and Lagos, where urban expansion has been strongly correlated with LST increases of up to 5°C over two decades (Nyamekye et al., 2022; Onyango et al., 2020).

The UHI results reinforce these observations by mapping the intensification of heat retention across the landscape. In 2010, high UHI values (12.75°C–15.10°C) were largely confined to urban cores, while cooler zones occurred in forested and water-influenced areas. By 2017, higher UHI values (16.57°C–19.20°C) extended into peri-urban belts, reflecting reduced vegetation and increased anthropogenic activities. By 2024, high UHI zones had expanded dramatically, with values reaching 25.70°C, leaving only small patches of cooler areas near water bodies. The persistence of relatively low UHI values near rivers and coastal towns such as Sakumono and Nungua underscores the importance of green and blue infrastructure in regulating microclimates. These findings corroborate Wemegah (2020), who emphasised the role of vegetation and water in moderating UHI intensity.

The implications of these findings are significant. The large-scale decline in vegetation undermines biodiversity and carbon sequestration while increasing communities' vulnerability to heat stress, flooding, and poor air quality. Rising LST and UHI intensities indicate an urgent need for climate-sensitive urban planning that incorporates green belts, urban forestry, and sustainable drainage systems. Without such interventions, urban residents face heightened risks of heat-related illnesses, and cities may experience surges in energy demand for cooling. This aligns with Biney et al. (2024), who stressed that thermal comfort in Ghanaian cities is increasingly at risk due to unchecked urban expansion and declining green spaces.

The observed transformations can largely be attributed to population growth, infrastructure expansion, and economic activities such as real estate development and land reclamation. The growth of peri-urban centres like Amasaman and Madina illustrates the spillover effect of Accra's expansion into formerly vegetated areas. Hydrological fluctuations in water bodies may also reflect irrigation, damming, and natural variability, a trend documented by Forkuor et al. (2020). While medium-resolution Landsat imagery provided a long-term perspective, it has limitations in detecting fine-scale heterogeneity, which future studies could address using Sentinel-2 or UAV-based data.

Overall, the findings provide compelling evidence that urbanisation in the study area has led to widespread vegetation decline, increased built-up surfaces, and marked rises in LST and UHI. These changes not only confirm global narratives of urban-driven climate modification but also highlight the urgent need for policy reforms and investment in urban greening strategies. National agencies such as the Lands Commission and the Environmental Protection Agency (EPA) of Ghana must prioritise frameworks that balance urban growth with ecological sustainability. Future research integrating socio-economic data and predictive modelling of UHI under climate change scenarios would further enhance understanding and provide actionable guidance for urban resilience.

## 6.0 Conclusions

This study has revealed a marked intensification of land surface temperature (LST) and the Urban Heat Island (UHI) effect in the Greater Accra Region from 2010 to 2024, with built-up areas expanding by nearly 67,850 hectares and vegetation declining by more than 40%. These findings confirm that rapid urbanisation, loss of vegetation, and the increase in impervious surfaces are the primary drivers of thermal stress in the city, while water bodies and residual green spaces help moderate localized temperatures. The novelty of this work lies in its comparative long-term analysis across three distinct periods, which not only quantifies the magnitude of land cover conversions but also tracks how rising heat has progressively shifted from central Accra into peri-urban towns. Unlike previous short-term assessments, this study provides evidence of spatially expanding vulnerability zones, making it a significant contribution to urban climate research in Ghana and West Africa.

Nonetheless, the study faced some limitations, including the use of medium-resolution Landsat imagery, which constrained fine-scale thermal detection, and the lack of socio-economic data integration that could directly link LST and UHI to population dynamics or energy demand. Despite these constraints, the results have important implications for planning and policy: the Environmental Protection Agency, Lands Commission, and metropolitan assemblies must prioritise ecological buffers, green infrastructure, and climate-resilient zoning to mitigate worsening UHI effects. Future research should employ high-resolution imagery, integrate demographic datasets, and test adaptive interventions such as green roofs, urban forestry, and sustainable land-use planning. Such measures are essential for reducing heat stress and fostering healthier, climate-resilient living conditions for Accra's growing urban population.

**Acknowledgement:** We thank the Greater Accra Metropolitan for making their land use plan and other reliable information available.

**Conflicts of Interest:** The authors declare no conflict of interest. They certify that they have no affiliations with or involvement in any organisation or entity with any financial or non-financial interest in the subject matter or materials discussed in this manuscript.

## References

- Aninakwah Isaac, A., Adu-Boahen, K., Edo, N., & Aninakwah, E. (2024). Analysis of trends in land utilisation and land cover dynamics in the Kwahu West Municipality, Ghana. *Journal of Asian Geography*, 3(1), 44–53. <https://doi.org/10.36777/jag2024.3.1.6>
- Aninakwah, E., & Aninakwah Isaac, A. (2025). Assessing the impacts of urban sprawl and encroachment on the Muni-Pomadze Lagoon ecosystem at Winneba, Ghana. *SN Social Sciences*, 5, Article 61. <https://doi.org/10.1007/s43545-025-01092-y>
- Aninakwah, E., Aninakwah Isaac, A., & Okyere, E. Y. (2025). Quantitative analysis of plastic waste accumulation in coastal Ghana: Implications for waste management. *Communication in Physical Sciences*, 12(2), 808–822. <https://doi.org/10.4314/cps.v12i2.11>
- Asori, M., & Adu, P. (2023). Modelling the impact of the future state of land use land cover change patterns on land surface temperatures beyond the frontiers of Greater Kumasi: A coupled cellular automaton (CA) and Markov chain. *Remote Sensing Applications: Society and Environment*, 29, 100967. <https://doi.org/10.1016/j.rsase.2023.100967>
- Asori, M., & Appiah, D. (2022). Land use/cover change and urban sprawl in Ghana. SSRN. <https://doi.org/10.2139/ssrn.4018888>
- Athukorala, D., & Murayama, Y. (2020). Spatial variation of land use/cover composition and impact on surface urban heat island in a tropical sub-Saharan city of Accra, Ghana. *Sustainability*, 12(19), 7953. <https://doi.org/10.3390/su12197953>
- Biney, E., Kwabena, E., Poku-Boansi, M., Hackman, K. O., Harris, E., Mensah, Y., Buston, D., Annan, E., & Elikplim, A. (2024). Analysing the spatio-temporal pattern of urban growth and its influence on urban heat islands in the Sekondi-Takoradi metropolis, Ghana. *Scientific African*, 26, e02366. <https://doi.org/10.1016/j.sciaf.2024.e02366>
- Biney, G. A., Darkwah, A. L., & Owusu, G. (2024). Urban expansion and land cover transitions in rapidly growing cities: Evidence from Accra, Ghana. *Sustainability*, 16(4), 2125. <https://doi.org/10.3390/su16042125>
- Borsah, A. A., Boah, E. A., & Brantson, E. T. (2025). Spatio-temporal land use/land cover change analysis and assessment of urban heat island in Ghana: A focus on the Greater Accra Region. *Journal of African Earth Sciences*, 221, 105474. <https://doi.org/10.1016/j.jafrearsci.2024.105474>
- Borsah, F. O., Ansah, A. S., & Opoku, P. (2025). Mapping urban land cover dynamics and heat island effects in West Africa. *Environmental Monitoring and Assessment*, 197(3), 112. <https://doi.org/10.1007/s10661-025-12245-1>
- Buo, I. N. K. (2019). Urban sprawl dynamics and urban heat islands (UHI) in Ghana (Master's thesis). University of Tartu.

- Devendran, A. A., & Banon, F. (2022). Spatio-temporal land cover analysis and the impact of land cover variability indices on land surface temperature in Greater Accra, Ghana, using multi-temporal Landsat data. *Journal of Geographic Information Systems*, 14(3), 240–258. <https://doi.org/10.4236/igis.2022.143013>
- Frimpong, B. F., Koranteng, A., & Opoku, F. S. (2023). Analysis of urban expansion and its impact on temperature utilising remote sensing and GIS techniques in the Accra Metropolis in Ghana (1986–2022). *SN Applied Sciences*, 5(8), 910. <https://doi.org/10.1007/s42452-023-05439-z>
- Gyasi-Addo, J. A. (2021). Evaluation of the effect of urbanisation on urban thermal behaviour using urban heat island indicators: The case of the CBD of Accra (Doctoral dissertation).
- Gyasi-Addo, J., & Bennadji, A. (2020). A procedure for assessing UHI intensity in the central business district of Accra. *Journal of Scientific Research and Reports*, 26(5), 42–61. <https://doi.org/10.9734/JSRR/2020/v26i530259>
- Hawley, A. H. (1950). *Human ecology: A theory of community structure*. Ronald Press.
- Mensah, C., Atayi, J., Kabo-Bah, A. T., Švik, M., Kyere-Boateng, R., Prempeh, N. A., & Marek, M. V. (2020). Impact of urban land cover change on the garden city status and land surface temperature of Kumasi. *Cogent Environmental Science*, 6(1), 1787738. <https://doi.org/10.1080/23311843.2020.1787738>
- Oke, T. R. (1982). The energetic basis of the urban heat island. *Quarterly Journal of the Royal Meteorological Society*, 108(455), 1–24.
- Park, R. E., Burgess, E. W., & McKenzie, R. D. (1925). *The city*. University of Chicago Press.
- Reagan, R., Agyepong, R., Morgan, E., Barimah, A., & Kofi, E. (2023). Trading greens for heated surfaces: Land surface temperature and perceived health risk in Greater Accra Metropolitan Area, Ghana. *Egyptian Journal of Remote Sensing and Space Sciences*, 26(4), 861–880. <https://doi.org/10.1016/j.ejrs.2023.09.004>
- Wemegah, C. (2020). Systematic assessment of urban heat island (UHI) warming in Greater Accra Region (Unpublished doctoral dissertation). <https://doi.org/10.13140/RG.2.2.11121.51040>
- Wemegah, C. S., Yamba, E. I., Aryee, J. N. A., Sam, F., & Amekudzi, L. K. (2020). Assessment of urban heat island warming in the Greater Accra Region. *Scientific African*, 8, e00426. <https://doi.org/10.1016/j.sciaf.2020.e00426>